Combined effects of reinforcement and prefabricated vertical drains on embankment performance

Allen Lunzhu Li and R. Kerry Rowe

Abstract: The behaviour of geosynthetic-reinforced embankments constructed over soft cohesive soils installed with prefabricated vertical drains (PVDs) is investigated by numerically examining an embankment constructed over different foundation soils. The partial consolidation during embankment construction, the consequent shear strength gain of the foundation soil, and the effect of the use of reinforcement on the mobilization of shear strength are examined. It is shown that the combined use of reinforcement and PVDs can significantly increase embankment stability and potentially allow the rapid construction of higher embankments than could be achieved with either method of soil improvement alone. Construction rate and spacing of PVDs can significantly affect the degree of consolidation at the end of construction and the stability of the embankment. For the situation examined, the effect of well resistance of typical vertical drains is insignificant. A relatively simple method for calculating the degree of consolidation and the strength gain of the foundation soil during construction is evaluated based on finite element results and is shown to be reasonably conservative. A design procedure is proposed to combine the design of reinforcement and PVDs.

Key words: soft clay, prefabricated vertical drain, reinforcement, embankment stability, consolidation, strength gain.

Résumé : Le comportement de remblais armés de géosynthétiques construits sur des sols mous cohérents équipés de drains verticaux préfabriqués (PVD) est étudié au moyen d'un examen numérique d'un remblai construit sur différents sols de fondation. On examine la consolidation partielle durant la construction du remblai, le gain de résistance au cisaillement du sol de fondation qui en découle, et l'effet de l'utilisation de l'armature sur la mobilisation de la résistance au cisaillement. Il est montré que l'utilisation combinée de l'armature et des PVD peut augmenter appréciablement la stabilité du remblai, et permettre potentiellement la construction rapide de remblais plus hauts que ceux qui pourraient être réalisés avec seulement l'une ou l'autre des méthodes d'amélioration. La vitesse de construction et l'espacement des PVD peuvent influencer appréciablement le degré de consolidation à la fin de la construction et la stabilité du remblai. Dans le cas étudié, l'effet de la résistance des drains verticaux est négligeable. Une méthode relativement simple de calcul du degré de consolidation et du gain de résistance du sol de fondation durant la construction est évaluée en partant des résultats d'éléments finis et s'est avérée être raisonnablement conservatrice. On propose une procédure de calcul pour combiner la conception de l'armature et des drains PVD.

Mots clés : argile molle, drains verticaux préfabriqués, armature, stabilité de remblai, consolidation, gain de résistance.

[Traduit par la Rédaction]

1. Introduction

Stability and the time required for consolidation are two major considerations in the design and construction of embankments over soft cohesive foundations having low bearing capacity and low hydraulic conductivity. Geosynthetic reinforcement has been widely used to improve the stability of embankments on soft clay soils (Humphrey and Holtz 1987; Fowler and Koerner 1987; Rowe and Soderman 1987*a*; Rowe 1997). In parallel, vertical drains have been used to shorten consolidation time of thick soft deposits by providing short horizontal drainage paths (Jamiolkowski et al. 1983). Due to the advantages of prefabricated vertical drains (PVDs) in terms of cost and ease of construction, they have almost entirely replaced conventional sand drains as vertical drains (Holtz 1987). The use of geosynthetic reinforcement in combination with prefabricated vertical drains has the potential to allow the cost-effective construction of substantially higher embankments in considerably shorter time periods than conventional construction methods (e.g., Lockett and Mattox 1987; Bassett and Yeo 1988; Schimelfenyg et al. 1990).

There has been considerable research examining the behaviour of reinforced embankments over soft foundations in terms of field behaviour (e.g., Rowe et al. 1984; Fowler and Edris 1987), in terms of theoretical behaviour as predicted using finite element methods (e.g., Rowe and Soderman 1987*b*; Hird and Kwok 1990; Chai and Bergado 1993; Rowe

Received January 10, 2001. Accepted April 25, 2001. Published on the NRC Research Press Web site at http://cgj.nrc.ca on January 10, 2002.

A.L. Li and R.K. Rowe.[1] Department of Civil Engineering, Ellis Hall, Queen's University, Kingston, ON K7L 3N6, Canada.

[1]Corresponding author (e-mail: kerry@civil.queensu.ca).

 DOI: 10.1139/cgj-38-6-1266

Fig. 1. The reinforced embankment, soft foundation, and vertical drains. GWT, groundwater table.

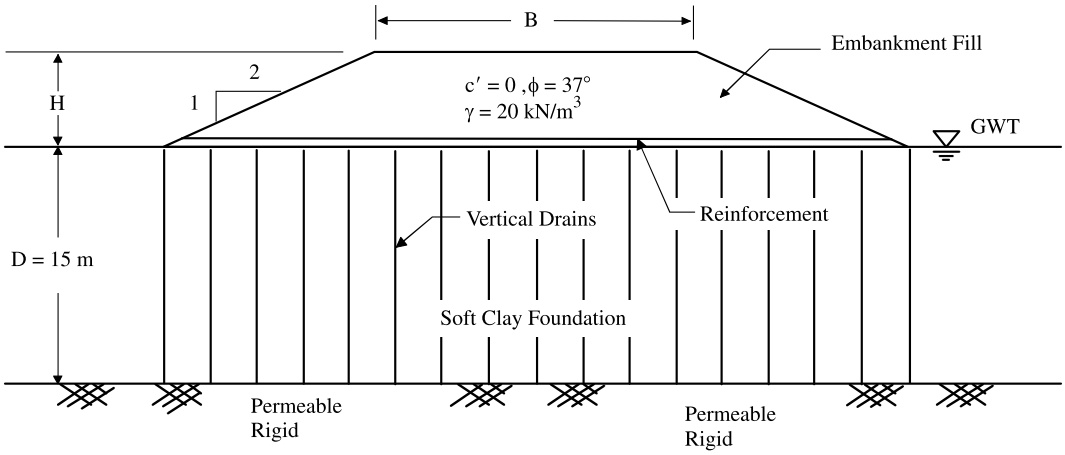

Fig. 2. Preconsolidation pressure and initial vertical effective stress profiles of soils A and B.

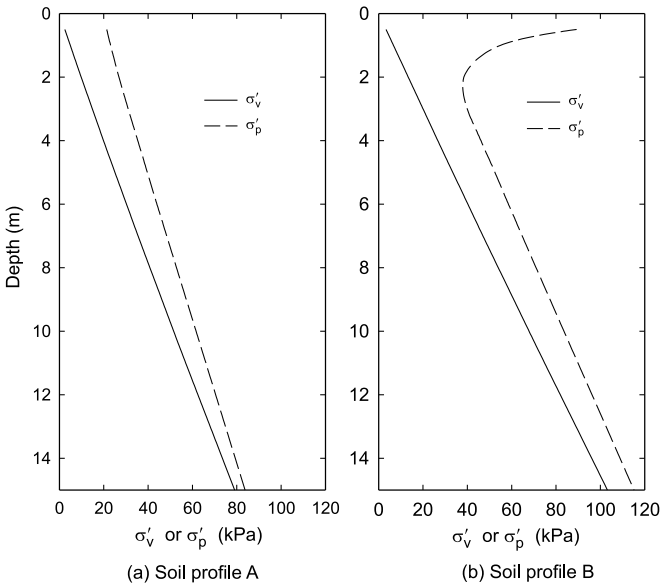

and Li 1999), and as observed in centrifuge model tests (e.g., McGown et al. 1981; Sharma and Bolton 1996). However, there has been a paucity of theoretical analyses examining the combined effects of reinforcement, vertical drains, and rate of construction on the embankment behaviour. Using a finite element technique, this paper examines combined effects of reinforcement and vertical drains on embankment stability and consolidation.

The design of reinforced embankments and vertical drains is usually treated separately in current design methods. A stability analysis is used in the design of reinforced embankments (e.g., Jewell 1982; Rowe 1984) and a consolidation analysis is used in the design of PVDs (e.g., Rixner et al. 1986; Holtz et al. 1991). The limit equilibrium method (Jewell 1982; Ingold 1982; Fowler and Koerner 1987; Bonaparte and Christopher 1987; Leshchinsky 1987; Mylleville and Rowe 1988; Koerner 1994; and others) has been widely adopted in practice for calculating the stability of reinforced embankments under undrained conditions. Although the assumption of undrained conditions is conservative for embankments on typical soft clays deposits, it neglects the significant effect of consolidation that may occur at typical rates of construction when the soil is overconsolidated during early stages of loading (Leroueil et al. 1978; Rowe et al. 1995; Li and Rowe 1999*a*; Leroueil and Rowe 2001), and especially when there are short horizontal drainage paths due to installation of vertical drains (Li and Rowe 1999*b*). However, the effects of partial drainage due to vertical drains on the stability of reinforced embankments have gained little attention and are not adequately addressed in current design methods. This paper shows that the effects of the reinforcement and PVDs are interrelated and should not be treated separately in design.

The present study considers the effects of both the reinforcement and the vertical drains simultaneously and investigates the combined benefits resulting from the partial consolidation of foundation soil due to PVDs and the basal reinforcement. The gain in shear strength of foundation soils due to partial consolidation during embankment construction is evaluated. The effect of the PVD spacing and well resistance is examined using a typical range of values. The effect of construction rate and stage construction sequence on stability and consolidation is also examined. The mobilized reinforcement strain is addressed for reinforced embankments over soft plastic soils under partially drained conditions. A new procedure which considers the effects of both reinforcement and vertical drains on the stability of embankments is proposed.

2. Problem considered and numerical model

The finite element program AFENA (Carter and Balaam 1990) was modified to incorporate soil reinforcement interaction, an elliptical cap soil model (Chen and Mizuno 1990; Rowe and Li 1999) coupled with Biot consolidation theory (Biot 1941), and a drainage element (Russell 1990) to model the well resistance of vertical drains.

This present study examines the construction of a highway embankment on a 15 m deep soft clay foundation underlain by a relatively rigid and permeable layer, as shown in Fig. 1. The finite element mesh (see Li and Rowe 2000) involved 1815 linear strain triangular elements, with 4003 nodes used to discretize the embankment and foundation soils. Two-

Table 1. Soil model parameters.

	Soil A	Soil B
Failure envelope slope, $M^*_{N/C}$	0.874	0.910
Friction angle (normally consolidated) (°)	27	28
Failure envelope slope, $M^*_{O/C}$	0.63	0.75
Cohesion intercept for overconsolidated clay, c_k (kPa)*	2.7–4.7	3.4–6.3
Aspect ratio, R	0.70	1.25
Compression index, λ	0.3	0.15
Recompression index, κ	0.030	0.025
Coefficient of earth pressure at rest, K_0'	0.6	0.6
Poisson's ratio, ν'	0.35	0.35
Average unit weight (kN/m^3)	15.2	16.7
Reference hydraulic conductivity, k_{vo} (m/s)	1×10^{-9}	1×10^{-9}
Reference void ratio, e_o	2.5	1.5
Hydraulic conductivity change index, C_k	0.5	0.5
Ratio of horizontal to vertical hydraulic conductivity, k_h/k_v	3	3

*In $\sigma_m' - \sqrt{2J_2}$ stress space, where σ_m' is the mean effective stress and J_2 is the second invariant of the deviatoric stress tensor.

noded bar elements were used for modeling the reinforcement and two-noded joint elements were used for both the embankment fill – reinforcement interface and the embankment fill – foundation interface (Rowe and Soderman 1987*a*). The centreline of the embankment and the far-field lateral boundary were taken to be smooth and rigid, with the lateral boundary located 100 m from the centreline. The bottom boundary of the finite element mesh was assumed to be rough and rigid. Consideration was given to the effect of a series of fully penetrating prefabricated vertical drains in a square pattern at three different spacings, S = 1, 2, and 3 m, equivalent to spacings of 1.07, 2.14, and 3.21 m, respectively, for a triangular pattern. Zero excess pore pressure was assumed along the drains to simulate ideal drains without well resistance. Two-noded drainage elements were used for vertical drains when the well resistance was considered. Embankment construction was simulated by turning on the gravity of the embankment in 0.75 m thick lifts at a rate corresponding to an embankment construction rate.

3. Model parameters

The parameters used in the finite element analyses reported in the subsequent sections of the paper are described in the following subsections.

3.1. Selection of foundation soil properties

Two soft foundations, denoted soils A and B, were examined. Soil A has a liquid limit of 76% and a plasticity index of 40%, and soil B has a liquid limit of 48% and a plasticity index of 30%. The vertical preconsolidation pressure, σ_p', profiles are shown in Fig. 2. Both clays were slightly overconsolidated, with overconsolidation ratios (OCRs) of 2.6–1.1 and 2.9–1.1, respectively, below the first 2 m. Soil B has a 2 m thick crust. The soil model parameters are summarized in Table 1. The first soil profile has an undrained shear strength, s_{uo}, of 5 kPa at the surface, increasing with depth at a rate, ρ_c, of 1.5 kPa/m; the second soil profile has an undrained shear strength, s_{uo}, of 20 kPa at the surface, decreasing to 10 kPa at 2 m depth, and then increasing at a rate, ρ_c, of 2.0 kPa/m. The stress ratio of undrained shear strength (under plane strain conditions) to preconsolidation pressure, $\alpha = s_u/\sigma_p'$, is 0.33 and 0.31 for soils A and B, respectively, in normally consolidated states.

The vertical hydraulic conductivity, k_v, of soft clays was taken to be a function of void ratio, e:

$$[1] \qquad k_v = k_{vo} \exp\left(\frac{e - e_o}{C_k}\right)$$

where k_{vo} is the reference hydraulic conductivity at the reference void ratio, e_o; and C_k is the hydraulic conductivity change index. The values for these parameters and the ratio of horizontal hydraulic conductivity, k_h, to vertical hydraulic conductivity, k_v, are summarized in Table 1. The initial average consolidation coefficient for soils A and B, respectively, is about 1.3 and 3.4 m^2/a in a normally consolidated state and 13.4 and 20.3 m^2/a in an overconsolidated state.

3.2. Embankment fill parameters and construction rates

The embankment fill was assumed to be a purely frictional granular soil with a friction angle ϕ' of 37° and a bulk unit weight γ of 20 kN/m^3. The dilatancy angle ψ was taken to be 6° based on the equation proposed by Bolton (1986). The nonlinear elastic behaviour of the fill was modelled using Janbu's (1963) equation:

$$[2] \qquad \frac{E}{P_a} = K\left(\frac{\sigma_3}{P_a}\right)^m$$

here E is the Young's modulus of the soil; P_a is the atmospheric pressure; σ_3 is the minor principal stress; and K and m are material constants selected to be 300 and 0.5, respectively, for typical fill materials.

A range of embankment construction rates (0.5–8 m/month) is examined in this paper.

3.3. Interface parameters and reinforcement stiffness

Rigid–plastic joint elements (Rowe and Soderman 1987*a*) were used to model the fill–reinforcement and fill–foundation

interfaces. The fill–reinforcement interface was assumed to be frictional, with $\phi' = 37°$ and cohesion intercept $c' = 0$. The fill–foundation interface had the same shear strength as that of the foundation soil at the ground surface. Reinforcement with tensile stiffness, J, varying from 250 to 2000 kN/m was examined.

3.4. Prefabricated vertical drains

The prefabricated drains modelled had a typical rectangular cross section of 100 mm × 4 mm (Holtz 1987) and were taken to be equivalent to a circular drain having a diameter d_w of 66 mm based on Kjellman (1948): $d_w = 2(b + t)/\pi$, where b and t are the width and thickness of the drain, respectively. The drain spacing, S, of 1, 2, and 3 m examined is within the typical spacing range used in practice (Holtz 1987). The effective diameter of drain influence was taken to be $D_e = 1.13S$ for a square configuration and $D_e = 1.05S$ for a triangular configuration (Rixner et al. 1986). The diameter of the smear zone, d_s, was assumed to be $d_s = 2d_m$ (Rixner et al. 1986), where d_m is the diameter of a circle with an area equal to the cross-sectional area of the mandrel. The mandrel d_m was assumed to be two times the drain diameter, d_w. The hydraulic conductivity of soil in the smear zone was assumed to be isotropic and the same as vertical hydraulic conductivity (i.e., 33% of the normal horizontal hydraulic conductivity). Both an ideal drain condition without well resistance and non-ideal drains with well resistance were examined.

Typical values of the discharge capacity, q_w, of many prefabricated drains are from 500 to 100 m^3/a (Holtz et al. 1991). As long as the discharge capacity is greater than 100–150 m^3/a under the confining pressures acting on the drain, there should be no significant decrease in the consolidation rate (Holtz 1987; Holtz et al. 1991). However, discharge capacity will decrease due to drain bending–folding and deterioration of the drain filter. Based on a review of test results for PVD products, the discharge capacity of some PVD products can be as low as 5–100 m^3/a under high confining pressures and low hydraulic gradients (Rixner et al. 1986; Holtz et al. 1991). Within this range, well resistance values of 5, 10, 25, 50, and 100 m^3/a for PVDs were examined.

4. The equivalent vertical drain in a plane strain problem

Strictly speaking, the analysis of a system involving discrete vertical drains should be conducted with a fully three-dimensional analysis, whereas most embankments are modelled for plane strain conditions. To avoid the need for a full three-dimensional analysis, some approximations are required to consider the vertical drains in a plane strain analysis. A number of authors (e.g., Cheung et al. 1991; Hird et al. 1992; Chai et al. 1995) have shown that vertical drains can be effectively modelled by using appropriate approximate methods to represent the typical arrangement of vertical drains in plane strain finite element analyses. The technique for matching a plane strain vertical drain system with an axisymmetric vertical drain system proposed by Hird et al. (1992, 1995) was adopted for the analyses reported in this paper. The theories on radial consolidation are well developed for different boundary conditions (Barron 1948; Kjellman 1948; Yoshikuni and Nakanodo 1974; Hansbo 1981; Zeng and Xie 1989). Hansbo's (1981) solution provides a relatively simple means of considering the effect of smear and well resistance, compares well with the solutions of Barron (1948) and Zeng and Xie (1989), and has gained wide acceptance (Jamiolkowski et al. 1983). As described here, this solution was used to check the finite element approximation adopted in the present study. For a cylindrical unit cell of soil influenced by a single drain under an instantaneous loading, the average degree of consolidation U_h on a horizontal plane at depth z and time t is given by Hansbo as

$$[3] \qquad U_h = 1 - \exp\left(-\frac{8T_h}{\mu}\right)$$

where $T_h = C_h t/4R^2$; $\mu = \ln(n/s) + (k/k_s)\ln(s) - 3/4 + \pi z(2l - z)k/q_w$; ratio $n = R/r_w$; ratio $s = r_s/r_w$; $q_w = \pi k_w r_w^2$; C_h is the horizontal consolidation coefficient; k, k_s, and k_w are the hydraulic conductivity of horizontal direction, soil in the smear zone and vertical drains, respectively; r_w, r_s, and R are the radius of the vertical drains, smear zone, and influence zone, respectively; and l is the length of the vertical drain. For plane strain conditions, Hird et al. (1992) show that $T_h = C_h t/4B^2$ and $\mu = 2/3 + 2z(2l - z)k/BQ_w$, where Q_w is the equivalent discharge capacity, and B is the half width of the influence zone for the plane strain unit cell. To match the average degree of consolidation at any time and any depth in these two cells, one can simply set U_{hpl} for a plane strain condition equal to U_{hax} for an axisymmetric condition (i.e., U_h in eq. [3]):

$$[4] \qquad U_{hpl} = U_{hax}$$

This can be achieved by any one of three methods: geometric matching, permeability matching, and a mix of geometric and permeability matching. Permeability matching involving adjusting the hydraulic conductivity of soil for plane strain conditions (k_{pl}) and putting $B = R$ is adopted in this paper. To satisfy eq. [4], the hydraulic conductivity and well resistance matching requirements are

$$[5] \qquad k_{pl} = \frac{2k_{ax}}{3\left[\ln\left(\frac{n}{s}\right) + \left(\frac{k_{ax}}{k_s}\right)\ln(s) - \frac{3}{4}\right]}$$

where k_{ax} is the hydraulic conductivity for the axisymmetric condition, and

$$[6] \qquad Q_w = \left(\frac{2}{\pi R}\right)q_w$$

For the vertical drain used in this paper having width b = 100 mm, thickness t = 4 mm, and ratio s = 4, the calculated ratio k_{pl}/k_{ax} is equal to 0.137, 0.120, and 0.112, respectively, for the influence radius R of 0.563, 1.125, and 1.688 m (i.e., S = 1, 2, and 3 m for a square configuration). Although the matching technique using Hansbo's (1981) solution is based on the assumption of an elastic soil and constant hydraulic conductivity, Hird et al. (1995) show that the matching technique also works well for consolidation involving plastic soil and variable hydraulic conductivity. To examine the accuracy of the matching procedure, a finite element analysis

Fig. 3. The variation of net embankment height with fill thickness.

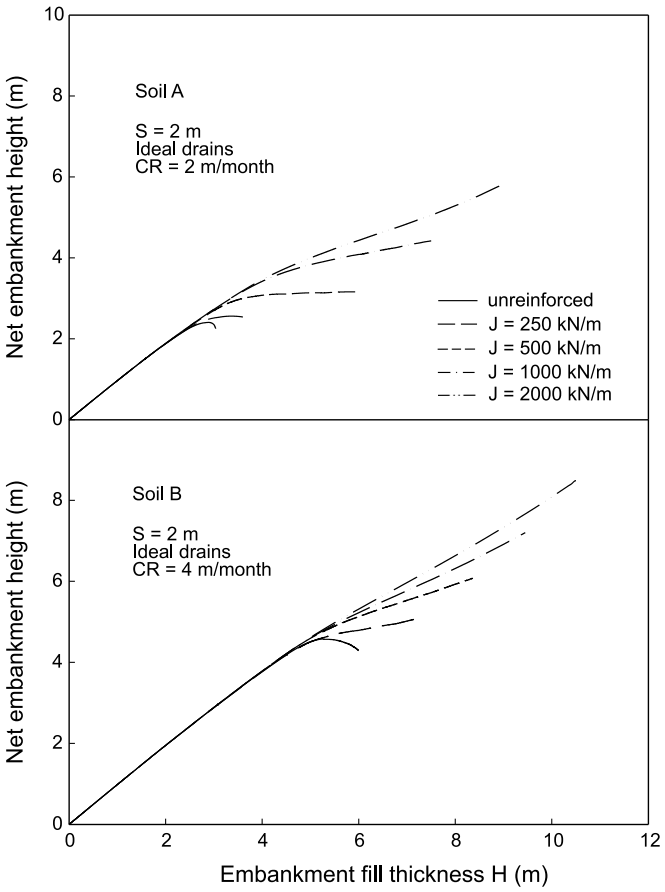

was conducted using both soil profiles for a unit cell of vertical drains with R = 1.125 m, and it was found that there was an excellent match between the plane strain and axisymmetric results (Li 2000).

5. Results and discussion

5.1. Effects of PVDs and reinforcement on embankment stability

The soil improvement involving the combined use of both PVDs and geosynthetic reinforcement has numerous advantages. The benefits of the use of PVDs are twofold (Holtz et al. 1991). The first is to accelerate the consolidation by shortening the drainage path and taking advantage of any naturally higher horizontal hydraulic conductivity of foundation soils. The second is to improve embankment stability due to the strength gain in foundation soils from the increase in effective stress associated with consolidation. Geosynthetic reinforcement provides additional embankment stability and tends to force the potential failure surface through soil with higher shear strength at depth in foundation deposits exhibiting a shear strength profile increasing with depth (Rowe and Soderman 1987*b*).

To study the combined effect of PVDs and reinforcement, finite element analyses were conducted to simulate embankment construction over soils A and B at a construction rate, CR, of 2 and 4 m/month, respectively. Figure 3 shows the variation of net embankment height (i.e., embankment fill thickness minus maximum settlement) with fill thickness. It is assumed here that the reinforcement could sustain the strains developed without breakage (the implication of this assumption will be examined shortly). The foundation soil was taken to be rate insensitive, isotropic, and not strain softening. For soil A, the unreinforced embankment could only be constructed to a height of 2.85 m. If reinforcement with tensile stiffness J = 250 kN/m was used, the failure height increased to 3.38 m. If reinforcement stiffness was greater than 500 kN/m, the embankment did not fail because the reinforcement provided enough resistance to allow the rate of shear strength gain of the foundation soil during construction to be fast enough to facilitate the rate of embankment loading. For soil B the unreinforced embankment failure height was 5.18 m. If reinforcement stiffness, J, was equal to or greater than 500 kN/m, the embankment did not fail due to bearing capacity failure at a construction rate of 4 m/month.

Even though, for reinforcement with $J \geq 500$ kN/m, the foundation did not experience a bearing capacity failure at these construction rates, a large yielded zone (i.e., where the soil was close to critical state) was found to be progressively growing beneath the embankment during construction. Consequently, the large plastic deformations, called progressive plastic deformations here, were developed in foundation soils during embankment construction. Due to these progressive plastic deformations, the reinforcement strain developed during construction could be much higher than the allowable strain of 4–7% (after reduction factors for creep, installation damage, and durability are applied; Industrial Fabrics Association International 1999). Under these circumstances, the maximum height to which the embankment could be constructed would be limited by the allowable reinforcement strain for a given type of reinforcement being considered. The slippage between soil and reinforcement was not observed in the finite element simulations for the cases examined. The cases with significantly weak soil-reinforcement planes where the slippage occurs before the allowable reinforcement strain is mobilized are not considered herein.

Figure 4 shows the embankment height corresponding to the tensile force mobilized at allowable reinforcement strains ranging from 4 to 7% for reinforcement with stiffnesses ranging from 250 to 2000 kN/m and embankments constructed over both foundation soils A and B, where zero force corresponds to unreinforced cases. The embankment height that is limited by the allowable reinforcement strains is called the maximum height or maximum embankment height here. For the unreinforced cases, the height corresponds to failure height. The use of reinforcement significantly increased the maximum embankment height compared with the unreinforced case for both soil profiles. For example, using a reinforcement with J = 2000 kN/m and an allowable strain of 6%, the maximum heights, H_ε, of 4.75 and 6.88 m were 67 and 33% above the failure height for an unreinforced embankment for soil profiles A and B, respectively. Figure 4 also shows the maximum height of an embankment over a foundation under undrained conditions for reinforcement having an allowable strain of 6% and stiffness ranging from 500 to 2000 kN/m. Comparing the undrained results with the partially drained results, it is evident that the shear strength gain during embankment construction arising from the use of vertical drains can result in a significant in-

Fig. 4. The maximum height H_ε of reinforced embankments with different reinforcement stiffnesses and allowable strains.

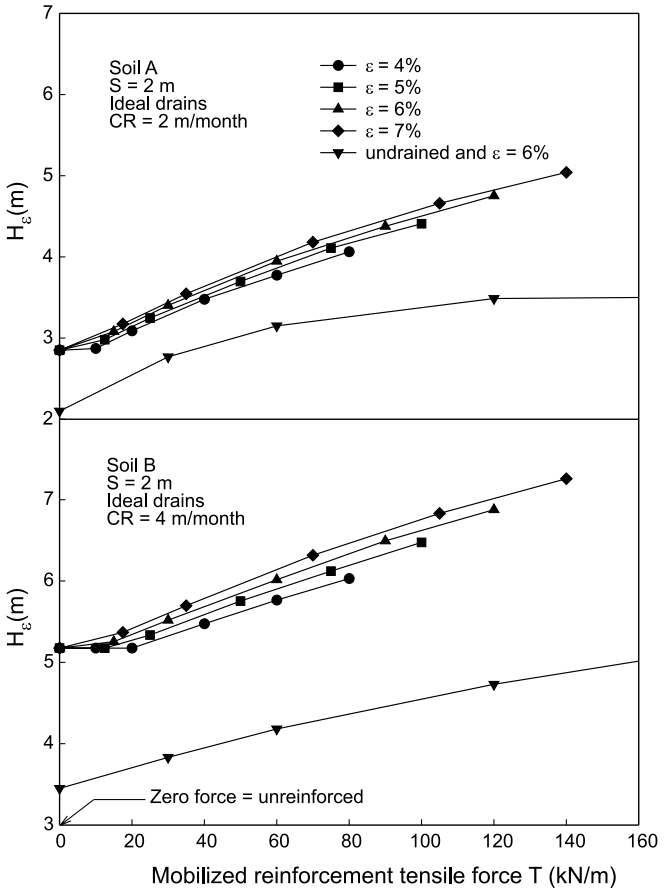

Fig. 5. The effect of construction rate on the stability of unreinforced and reinforced (J = 1000 kN/m) embankments.

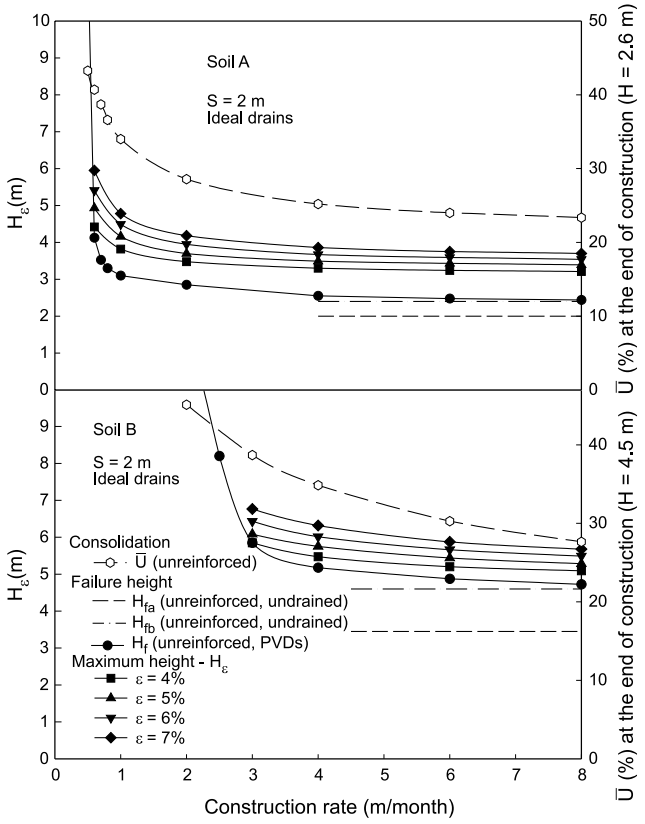

crease in maximum embankment height. For example, using a reinforcement with J = 2000 kN/m and an allowable strain of 6%, the maximum heights, H_ε, for the partially drained cases with PVDs were 36 and 45% above that of the undrained cases for soils A and B, respectively.

5.2. Effects of embankment construction rate and partial consolidation during construction

Figure 5 shows the variation of maximum height with construction rate for both reinforced (with J = 1000 kN/m) and unreinforced embankments. It is evident that the embankment stability was sensitive to the construction rates examined. It was found that there was a threshold construction rate for the unreinforced embankment below which the embankment would not fail due to bearing capacity failure of foundation soil. As shown in Fig. 5, the threshold rate was about 0.5 and 2 m/month for soils A and B, respectively. This implies that if construction was controlled at a rate slower than the threshold rate, reinforcement was not needed to maintain embankment stability. The use of reinforcement could efficiently increase embankment stability only when the construction rate was greater than the threshold rate. The increase in stability with the decrease in construction rate resulted from the rate of consolidation and the consequent strength gain at the end of construction. The rate of consolidation of the foundation soil at the end of construction can be represented in terms of the average degree of consolidation, $\overline{U}$, below the embankment centre. Figure 5 shows the variation of $\overline{U}$ at the end of construction with construction rate for two unreinforced embankments (i.e., H = 2.6 and 4.5 m) over soils A and B. The degree of consolidation at the end of construction significantly increased with a decrease in construction rate when the rate was approaching or slower than the threshold rate.

Figure 5 also shows the unreinforced embankment failure heights: (*i*) H_{fa}, using the initial undrained shear strength profiles of the soils (see Fig. 2); and (*ii*) H_{fb}, using the strength profiles of soils in normally consolidated states (assuming that current effective vertical stresses were equal to preconsolidation pressures), calculated by $s_u = \alpha\sigma'_p$, where σ'_p is the initial preconsolidation pressure and α is 0.33 and 0.31 for soils A and B, respectively (see Sect. 3.1.). Both H_{fa} and H_{fb} were calculated using limit equilibrium methods. It is noted that when the construction rate increased, the decrease in failure height of the unreinforced embankment diminished to an asymptotic value H_{fb} corresponding to the undrained shear strength of soils in normally consolidated states, $s_u = \alpha\sigma'_p$.

For reinforced embankments, the maximum height followed the same trend with construction rate as that of the failure height for unreinforced embankments; however, the maximum height was also governed by allowable reinforcement strains. At lower construction rates, the embankment stability was governed by the partial consolidation during construction. At higher construction rates, the reinforcement did significantly increase the maximum embankment height.

Fig. 6. The effect of construction rate on the deformations of foundation soil A and the maximum reinforcement strain.

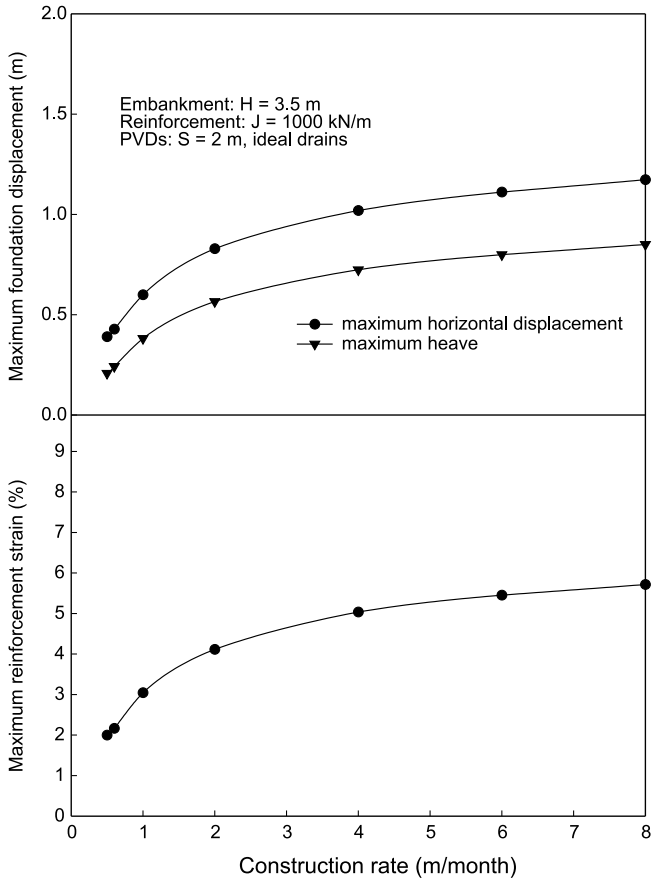

Fig. 7. The variation of the maximum height $H_{\varepsilon = 5\%}$ with reinforcement tensile stiffness at different construction rates and reinforcement stiffnesses.

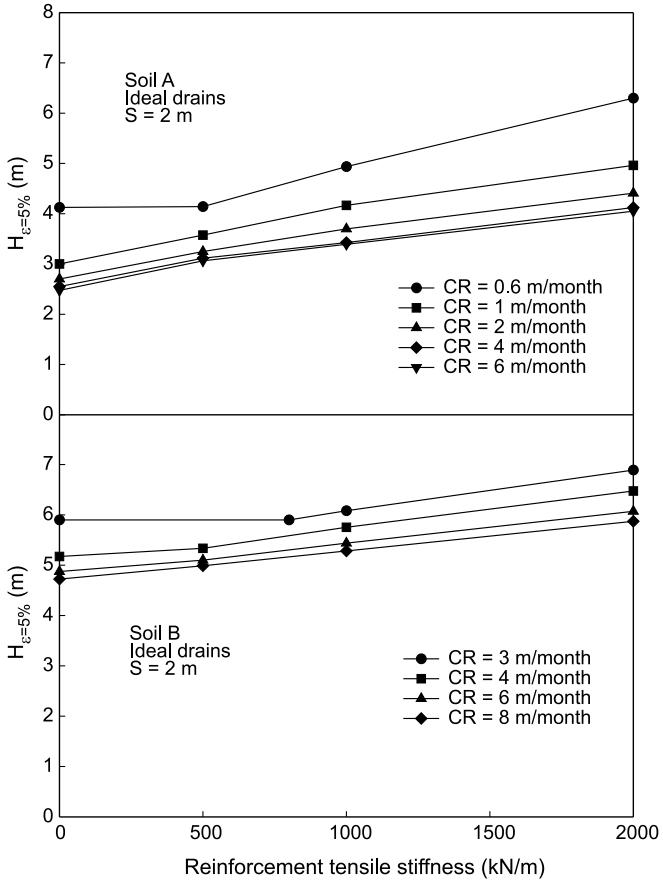

Figure 6 shows the variation of foundation deformation and reinforcement strain with construction rate for a 3.5 m high embankment constructed over foundation soil A. A slower construction rate resulted in less foundation shear deformations and reinforcement strains, especially when the construction rate was slower than 2 m/month for this particular case. Figure 6 indicates that the excessive horizontal deformations of foundation soils, heave at the embankment toe, and reinforcement strains can be prevented by controlling the construction rate.

5.3. Effects of reinforcement stiffness for embankments constructed at different rates

The reinforcement stiffness can be an important factor affecting embankment stability under partially drained conditions when the construction rate is faster than the threshold rate, as shown in Fig. 7. The maximum height corresponding to an allowable maximum reinforcement strain of 5% is plotted against reinforcement stiffness for different construction rates. The results plotted for $J = 0$ correspond to the unreinforced case. It is evident that above construction rates of 0.5 and 2 m/month for soils A and B, respectively, stiffer reinforcement will permit the construction of a higher embankment.

5.4. Effects of spacing of vertical drains

From the classical consolidation theory, it is well known that the rate of consolidation is inversely proportional to the square of the length of the drainage path. Three configurations of PVD system with spacing of 1, 2, and 3 m were examined to investigate the effect of spacing on embankment stability over soil A. The threshold construction rate for unreinforced embankments was calculated to be 2, 0.5, and 0.2 m/month for PVD spacings of 1, 2, and 3 m, respectively. Figure 8 shows the variation of maximum embankment height for an allowable strain of 5%, $H_{\varepsilon = 5\%}$, with reinforcement stiffness at different construction rates for soil A with PVD spacings of 1 and 3 m. Comparing the embankment heights for $S = 1$, 2, and 3 m (Figs. 7, 8), the improvement in stability due to a change in spacing from 2 m to 1 m was much greater than that observed where the spacing was changed from 3 m to 2 m. For example, at 4 m/month and $J = 2000$ kN/m, $H_{\varepsilon = 5\%}$ is 5.71, 4.12, and 3.96 m at spacings of 1, 2, and 3 m, respectively. The reason for this is that the vertical drain spacing significantly influences the degree of consolidation at the end of embankment construction, and consequently the shear strength gain during construction. For example, at the end of construction of a 3.75 m high embankment on foundation soil A at a rate of 4 m/month, the average degree of consolidation under the embankment centre was about 37, 24, and 21% for spacings of 1, 2, and 3 m, respectively.

5.5. Effects of well resistance of vertical drains

Figure 9 shows the variation in maximum height for the range of discharge capacities of PVDs with a 2 m spacing

Fig. 8. The effect of PVD spacing on the embankment stability.

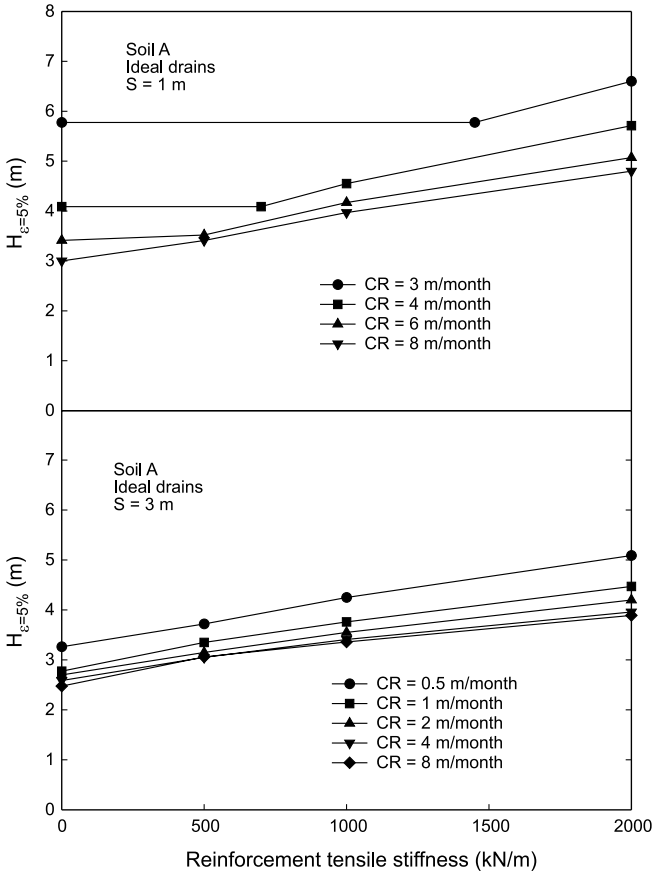

Fig. 9. The effect of discharge capacity on the embankment stability and consolidation at the end of construction.

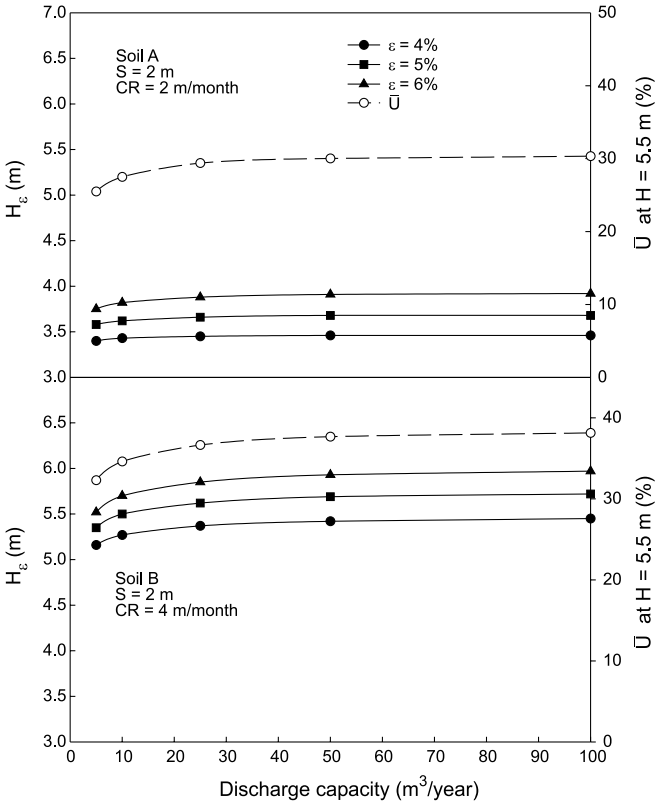

for embankments constructed at 2 m/month over soil A and 4 m/month over soil B. When the discharge capacity was 10 m^3/a (or greater), for soil A, the effect of well resistance on embankment stability was insignificant. The effect was somewhat greater for the stiffer soil B, but still small for discharge capacities as low as 10 m^3/a. For a discharge capacity greater than 50 m^3/year, there was no practical effect of well resistance on the maximum embankment height for either soil A or soil B. The effect of well resistance on embankment stability can be explained by examining the degree of consolidation at the end of construction. Figure 9 also shows the average degree of consolidation at the end of construction of 3.75 and 5.5 m high embankments over soils A and B, respectively. The variation of maximum height with discharge capacity is reflected by the variation of consolidation. Typical values of the discharge capacity of many PVDs are over 50 m^3/a and around 100–500 m^3/a (Rixner et al. 1986; Holtz et al. 1991). Therefore, the well resistance of many PVD products theoretically does not affect the stability of embankments for the typical soil profiles examined as indicated in Fig. 9. However, the effect of well resistance needs to be further investigated when drains are very long and lateral stresses are high, or if the drains are susceptible to folding and (or) deterioration.

5.6. Effects of two-stage construction

Since shear strength gain may be significant in relatively short periods of time after construction due to the fast rate of consolidation when vertical drains are used, stage construction methods are often employed to construct an embankment to the design grade. In this section, stage construction methods were simulated for reinforced embankments (with reinforcement stiffness values between 250 and 2000 kN/m) constructed over soils A and B. During the first stage, the reinforced embankments were constructed to a height of 2 m over soil A at a rate of 2 m/month and a height of 3.5 m over soil B at a rate of 4 m/month. Figure 10 shows the variation in maximum embankment height H_ε at the second stage with mobilized tensile force at different allowable strains for soils A and B.

For soil A, the second stage was initiated after 4 months of consolidation to reach an average degree of consolidation of 62%. The average increase in maximum height of reinforced embankments related to one-stage construction was about 0.64 m, which was not particularly significant because the increase of shear strength of the foundation soil could not be fully mobilized due to the constraint of the allowable reinforcement strains. However, if one was to build a higher embankment at the first stage for the case with a stiffer reinforcement, the benefit of two-stage construction would be more pronounced due to the greater shear strength gain of the foundation soil under the higher embankment load. For example, if a reinforced embankment (with J = 2000 kN/m and ε_{all} = 5%) was constructed to H = 3.5 m over soil A during the first stage, after 4 months of consolidation, the embankment could be constructed to a maximum height of 5.63 m during the second stage, with a net increase of 1.22 m (an increase of 28%) relative to the maximum height of one-stage construction.

Fig. 10. The variation of embankment maximum height with reinforcement tensile force for two-stage construction.

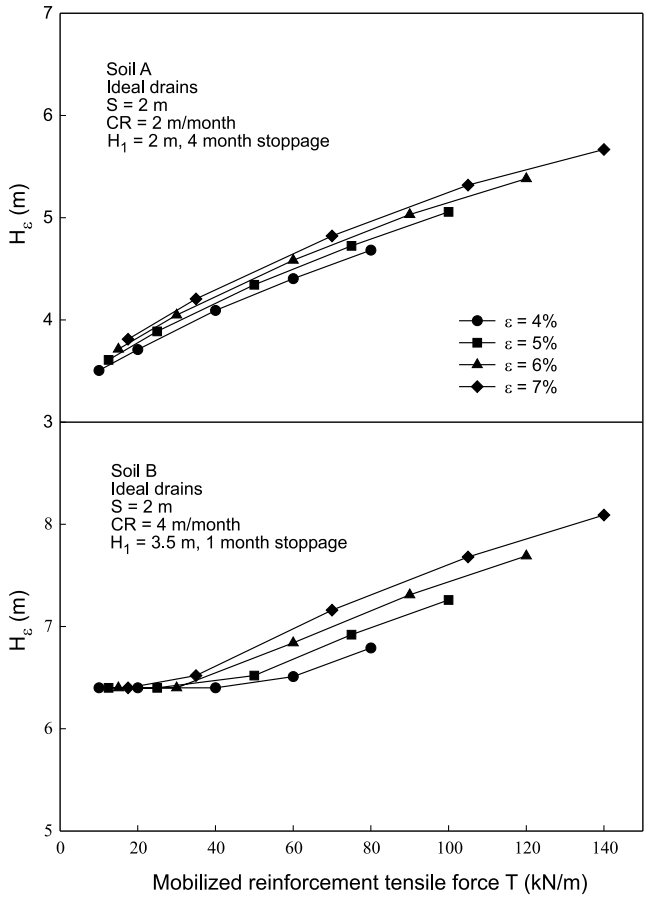

For soil B, the second stage was initiated after 1 month of consolidation to reach an average degree of consolidation of 55%. The maximum height of reinforced embankments during the second stage is shown in Fig. 10. For reference, the failure height of the unreinforced embankment was 6.4 m and represented the lowest maximum height. The increase in embankment height relative to that for one-stage construction was in the range of 0.8–1.2 m for the reinforcement stiffness values and allowable strains considered. An alternative to the use of stiff reinforcement to allow construction to a greater embankment height would be to achieve a greater strength gain of the foundation soil by extending the time for consolidation between construction stages. For example, if the stoppage at H = 3.5 m was extended from 1 month to 4 months, the calculated unreinforced embankment failure height was over 9.5 m during the second stage of construction. Therefore, reinforcement was not necessary to achieve a design grade equal to or below 7.0 m in terms of stability (with a minimum factor of safety of 1.3). Nevertheless, the use of reinforcement was found to reduce the shear deformation of foundation soils.

Similar to the case of one-stage construction (see Fig. 4), Fig. 10 shows that during two-stage construction the higher the reinforcement force, the higher the allowable strain, and the greater the maximum embankment height that can be achieved.

Fig. 11. The variation of maximum reinforcement strain with fill thickness.

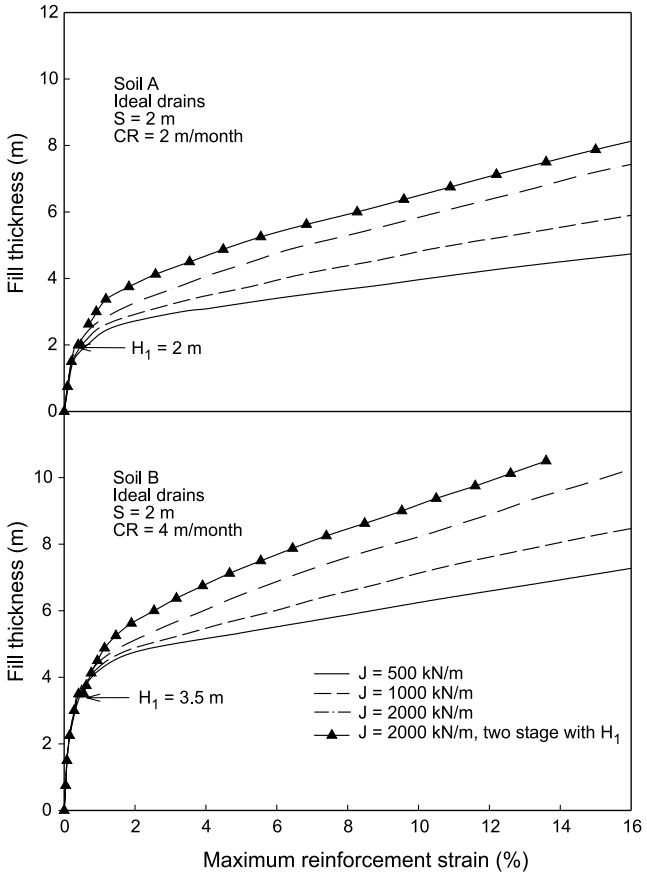

From the foregoing findings, it is evident that for a two-stage construction sequence it is desirable to build the embankment as high as possible during the first stage, by using reinforcement, so that the maximum amount of strength gain of the foundation soil can occur during the construction stoppage. Furthermore, as indicated by Li and Rowe (1999*a*), the use of reinforcement can also possibly reduce the number of stages required for a multistage construction sequence. To safely construct an embankment to a design grade and achieve a maximum degree of consolidation within a limited period of time, it is necessary to have a design method that can readily accommodate the change of the configuration of both reinforcement and PVDs and construction sequences.

5.7. Reinforcement strain

Figure 11 shows the variation of maximum reinforcement strain with embankment fill thickness for both one-stage and two-stage construction, assuming that the reinforcement could sustain the strain developed without breakage. In Fig. 11, H_1 is the fill thickness at the first stage of construction (i.e., 2 and 3.5 m over soils A and B, respectively). During the early stage of construction, the maximum reinforcement strain for all cases was small and within 1% when the foundation deformed, mainly elastically. But then it increased significantly when the embankment loading caused large plastic deformations of the foundation as the fill thickness exceeded the failure height of the unreinforced embankment (i.e., 2.85 and 5.18 m for

Fig. 12. Contours of strength gain Δs_u (kPa) at the end of construction from finite element analyses.

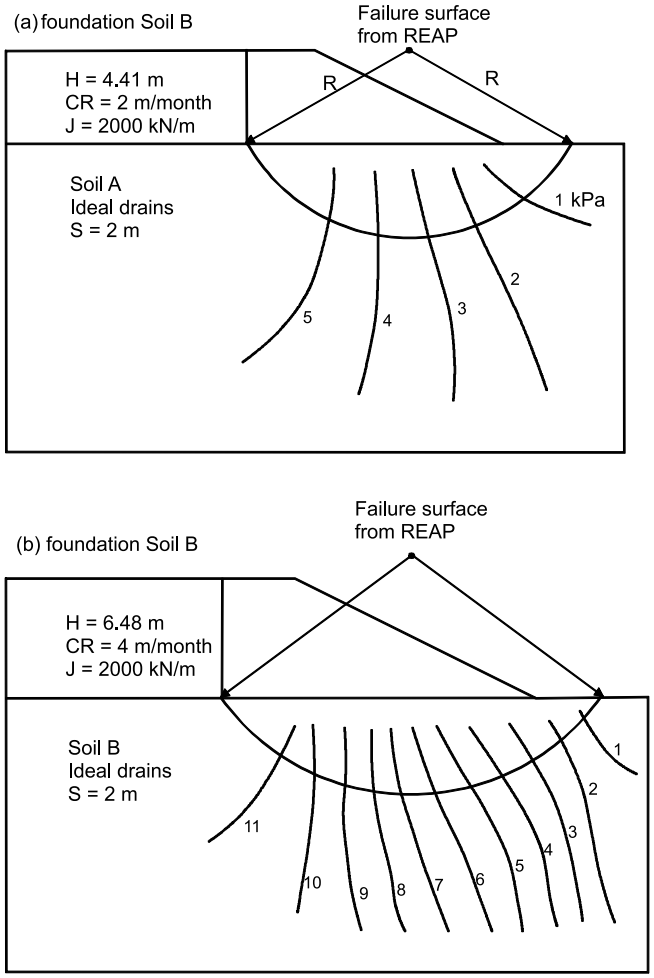

soils A and B, respectively). After the initial, mainly elastic, deformations were developed, the stiffer reinforcement resulted in smaller reinforcement strains for a given fill thickness. This effect of reinforcement stiffness was more significant for embankments over soil B (the stronger soil) than for embankments over soil A. In all cases, the embankment did not fail due to bearing capacity failure of foundation soil, even though very high reinforcement strain was developed. The increase in embankment height at very high reinforcement strain levels was attributed to the increase in shear strength of the foundation soil due to partial consolidation during construction.

Comparing two-stage construction with one-stage construction for the cases with reinforcement stiffness J = 2000 kN/m, it is evident that the additional strength gain resulting from consolidation during the stoppage caused less reinforcement strain in the second stage for a given embankment height. It was also found that the higher embankment during the first stage and the longer the stoppage, the greater the stiffening effect and the lower the strain that was developed when a significant amount of additional fill was placed. For clarity, the results from the cases with a higher embankment and longer stoppage at the first stage are not plotted in Fig. 11.

It is evident from Fig. 11 for both one-stage and two-stage construction that the stiffer the reinforcement and (or) the higher allowable reinforcement strain, the greater the fill height that can be achieved. Figure 11 also shows that during the stoppage between the two construction stages the consolidation settlement of the foundation soils under the relatively low embankments has an insignificant effect on the reinforcement strain. However, Li (2000) has shown that the long-term differential settlement of foundation soils under relatively high embankments can significantly increase the mobilized reinforcement strain and force.

5.8. Consolidation during embankment construction and shear strength gain

Significant consolidation of foundation soils may occur during embankment construction because of the high consolidation coefficient of initially overconsolidated soils (Leroueil et al. 1978; Rowe and Li 1999; Leroueil and Rowe 2001) and the short horizontal drainage path provided by PVDs (Li and Rowe 1999*b*). To evaluate the consolidation and consequent shear strength gain during construction, two embankments with heights H = 4.41 and 6.48 m over soils A and B, respectively, and reinforcement with tensile stiffness J = 2000 kN/m and allowable strain ε_{all} = 5% were examined. The average excess pore pressure dissipation in foundation soils under the embankment centre at the end of construction was 31 and 40% for embankment heights H = 4.41 and 6.48 m, respectively.

Figure 12 shows the contours of the increase in undrained shear strength Δs_u of the foundation soil during construction for both embankments. For the sake of clarity, Fig. 12 does not include the increase in undrained shear strength near the top and bottom layers, where the gradient of shear strength increase is high due to the drainage boundary effects. The undrained shear strength, s_u, was calculated at each integration point in the finite element analysis based on the effective stresses at the end of construction, and then s_u was averaged along the horizontal direction within the influence zone of each PVD. Due to the presence of the PVDs, the increase of undrained shear strength Δs_u (i.e., s_u at the end of construction minus initial undrained shear strength, s_{uo}) was rather uniform throughout the thickness of the deposit, even though the initial undrained shear strength increased with depth at a rate of ρ_c (see Sect. 3.1.). The increase in shear strength of soil under the embankment centre (5 kPa for soil A and 11 kPa for soil B) was higher than that under the embankment slope (i.e., about 3 kPa for soil A and 6.5 kPa for soil B). Figure 12 also shows the calculated potential failure surface using the limit equilibrium program (REAP). It is evident that the increase in shear strength along the failure surface had the highest magnitude at locations below the embankment crest and gradually dropped to practically no increase (<1 kPa) beyond the embankment toe.

5.9. Design considerations for consolidation and strength gain of foundation soil

Finite element results in previous sections have shown that the consolidation and consequent strength gain of foundation soil at the end of construction is significant, particularly when the construction rate is slow. These results imply that the assumption of undrained loading is too conservative

Fig. 13. Linear ramp load function for the consolidation analysis considering the soil in its overconsolidated and normally consolidated states.

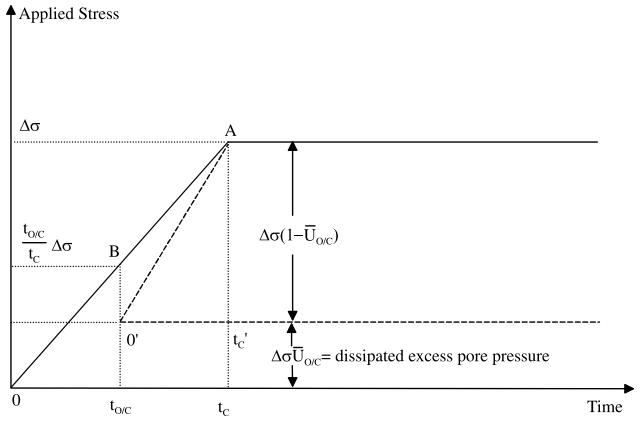

for the cases having vertical drains installed in foundation soils. The significant consolidation during construction is a result of two factors, namely the high consolidation coefficient of foundation clay in its initial overconsolidated state, and the time-dependent loading. Classical consolidation theories are unable to predict the effect of these two factors due to their limitations, as discussed by Mesri and Rokhsar (1974), Olson and Ladd (1979), and Holtz et al. (1991). To take these two factors into account, the conventional consolidation theories should be modified without making them too complicated for practical use.

The theory proposed by Mesri and Rokhsar (1974) can consider the change of compressibility of clay from overconsolidated states to normally consolidated states for one-dimensional consolidation problems. However, the governing equations must be solved using a numerical technique, which may not be readily available for design in many cases. As the consolidation of vertical drains is usually calculated in terms of average degree of consolidation, the authors suggest the following simple approximate method to calculate the average degree of consolidation to consider the fast dissipation of excess pore pressure during the early stage of embankment construction when the soil is in an overconsolidated state. All assumptions of Terzaghi's consolidation theory are preserved except for the change in compressibility as a soil moves from the overconsolidated to normally consolidated state and the time-dependent loading. It is assumed that the soil becomes normally consolidated when the average degree of consolidation at a particular time is such that the average vertical effective stress of soils along the drainage paths is equal to the preconsolidation pressure. At this time, the change of soil compressibility is a step change (i.e., from recompression index C_r to compression index C_c). The time-dependent loading is taken to be a linear ramp loading.

The proposed method is shown conceptually in Fig. 13. A stress of $\Delta\sigma$ is applied during a period of time t_C (from point O to point A in Fig. 13). During the period to time $t_{O/C,}$ when the soil is overconsolidated, the consolidation is governed by consolidation coefficient $C_{O/C}$; after $t_{O/C}$, when the soil becomes normally consolidated, the consolidation is governed by consolidation coefficient $C_{N/C}$. For a foundation deposit under a two-way drainage condition, the average degree of consolidation at any time is defined as

$$[7] \qquad \overline{U} = \frac{2H\Delta\sigma(t) - \int_0^{2H} u\,dz}{2H\Delta\sigma}$$

where H is the drainage distance (i.e., the half thickness of the foundation deposit), $\Delta\sigma(t)$ is the applied stress at time t, and u is the excess pore pressure at time t. At time $t_{O/C}$, the applied stress $\Delta\sigma(t)$ is equal to $\Delta\sigma t_{O/C}/t_C$, the average degree of consolidation is $\overline{U}_{O/C}$ for a total stress of $\Delta\sigma$, and the average change in effective stress at this time is $\Delta\sigma\overline{U}_{O/C}$. The excess pore pressure that will need to dissipate after application of the full stress $\Delta\sigma$ is $\Delta\sigma(1 - \overline{U}_{O/C})$, and it is assumed that this excess pore pressure is developed over a period of time $t'_C = t_C - t_{O/C}$. After time $t_{O/C}$, the average consolidation, $\overline{U}_{N/C}$, is calculated using $C_{N/C}$ for the ramp load of $\Delta\sigma(1 - \overline{U}_{O/C})$. The proposed approximation is shown graphically in Fig. 13, with the linear load function 0–A being replaced by two linear load functions: 0–B and 0′–A for soil in overconsolidated and normally consolidated states, respectively. It is assumed that the average degree of consolidation under the load 0–A after $t_{O/C}$ is equivalent to the average degree of consolidation under the load 0′–A plus the average degree of consolidation under the load 0–B at time $t_{O/C}$. Namely, the total average degree of consolation at time t ($\geq t_{O/C}$) is

$$[8] \qquad \overline{U} = \overline{U}_{O/C} + (1 - \overline{U}_{O/C})\overline{U}_{N/C}$$

To consider the consolidation of soil under a time-dependent loading, a number of methods have be proposed (e.g., Taylor 1948; Schiffman 1958; Olson 1977; Zhu and Yin 1998, 1999). Olson (1977) derived relatively simple solutions considering both vertical and radial drainage for a linear ramp loading problem based on the assumptions of the classic consolidation theories except time-dependent loading. The equations for vertical consolidation are as follows:

$$[9a] \qquad T \leq T_c; \quad \overline{U}_v = \frac{T}{T_c}\left\{1 - \frac{2}{T}\sum\frac{1}{M^4}[1 - \exp(-M^2T)]\right\}$$

$$[9b] \qquad T \geq T_c; \quad \overline{U}_v = 1 - \frac{2}{T_c}\sum\frac{1}{M^4}[\exp(M^2T_c) - 1]\exp(-M^2T)$$

where T is the time factor for vertical consolidation; T_c is the time factor at the end of construction; and $M = \pi(2m + 1)/2$, for $m = 0, 1, 2, 3, \ldots$ until the sum of all remaining terms is insignificant. The equations for horizontal (radial) consolidation are as follows:

$$[9c] \qquad T_h \leq T_{hc}; \quad \overline{U}_h = \frac{1}{T_{hc}}\left\{T_h - \frac{1}{A}[1 - \exp(-AT_h)]\right\}$$

$$[9d] \qquad T_h \geq T_{hc}; \quad \overline{U}_h = 1 - \frac{1}{AT_{hc}}[\exp(AT_{hc} - 1)]\exp(-AT_h)$$

where T_h is the time factor for horizontal consolidation; T_{hc} is the time factor at the end of construction; and $A = 8/\mu$ (where μ is defined in Sect. 4) using Hansbo's (1981) solution for vertical drains.

Fig. 14. Comparison of calculated average degree of consolidation for a unit cell of vertical drain system in soil A using different methods (including both vertical and horizontal drainage). FEM, finite element method.

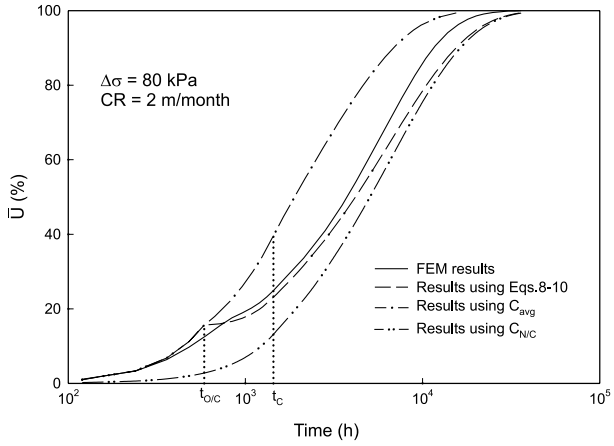

The equation for combined vertical and radial consolidation using the method of Carrillo (1942) is as follows:

$$[10] \quad \overline{U} = 1 - (1 - \overline{U}_h)(1 - \overline{U}_v)$$

To examine eqs. [8]–[10], Fig. 14 shows the predicted average degree of consolidation for a unit cell of a vertical drain system in a 15 m thick foundation soil A (including both vertical and horizontal drainage) under a one-dimensional loading condition using the finite element method and the proposed analytical method. Also shown is the calculated average degree of consolidation based on the consolidation coefficient, $C_{N/C}$, for soil in its normally consolidated state and based on the average consolidation coefficient, C_{avg}, at time t which is an average value of $C_{O/C}$ and $C_{N/C}$ weighted by the increase in effective stress at time t. The finite element results are calculated from a simulation of an axisymmetric vertical drain. It is evident that the prediction of consolidation using eq. [8] is conservative after time t_C and compares well with finite element results, especially at the end of construction. The method using $C_{N/C}$ significantly underestimates the consolidation during the early stage of loading, and the method using an average of $C_{O/C}$ and $C_{N/C}$ significantly overpredicts the consolidation, hence these methods are not suitable for use.

Equations [8]–[10] can be used to estimate the average degree of consolidation of the foundation soil and the consequent average shear strength gain of foundation soils. As shown in Fig. 12, the variation of the strength gain of foundation soil with depth is relatively uniform for a relatively uniform foundation soil, and the magnitude of strength gain for soil along the failure surface gradually decreases from a maximum below the embankment crest to a minimum in front of the embankment toe. The following simple procedure is used to predict the strength gain in foundation soils with PVDs as shown by finite element results. Since the average degree of consolidation is calculated over the depth of the soil stratum through which vertical drains penetrate, the soil parameters can be averaged over the depth of foundation in the following calculations.

Assuming that the embankment loading is one-dimensional, the increase in undrained shear strength of soil below the embankment centre, Δs_{uc}, can be estimated based on the SHANSEP method (Ladd and Foott 1974) by

$$[11] \quad \Delta s_{uc} = [\alpha(\sigma'_{vo} + H\gamma_{fill}\overline{U})] - s_{uo}$$

where the ratio $\alpha = s_u/\sigma'_p$ is constant for a given soil; σ'_{vo} and s_{uo} are the initial vertical effective stress and undrained shear strength, respectively, prior to embankment construction; and γ_{fill} is the unit weight of the embankment fill.

In the SHANSEP method, the undrained shear strength of clay is normalized to the vertical effective stress, and strength gain is usually estimated by evaluating the increase in vertical effective stress (Ladd 1991). For locations below the embankment centre, this normalization works reasonably well, since a K'_0 consolidation condition is representative for these locations, where K'_0 is the coefficient of lateral earth pressure at rest. However, for the locations along the failure surface below the embankment slope, the loading imposed by the embankment is at least two-dimensional and the consolidation may not be well approximated by K'_0 consolidation. The proposed method uses the undrained shear strength normalized to the effective mean stress, σ'_m, for locations along the failure surface, assuming that the ratio $\beta = s_u/\sigma'_m$ is constant for a given soil in its normally consolidated state. This is based on the fact that the shear strength of soil is governed by three-dimensional effective stresses. For simplicity, the strength gain is evaluated only by examining the change in effective mean stress, and the effect of change in deviatoric stresses on strength gain is neglected.

When soil is in its normally consolidated state, the effective mean stress $\sigma'_m = [(1 + 2K'_0)/3]\sigma'_p$. Therefore, β is calculated by

$$[12] \quad \beta = \frac{3}{1 + 2K'_0}\alpha$$

where K'_0 is the coefficient of lateral earth pressure at rest for soil in its normally consolidated state.

The increase in three-dimensional stress due to the embankment loading can be estimated using an influence factor, I_q, for total mean stress σ_m based on elastic solutions (e.g., Poulos and Davis 1974), and I_q can be averaged over the potential slip surface. The average degree of consolidation of soils along the potential failure surface, $\overline{U}_f$, is calculated separately from that of soil below the embankment centre based on the fact that the degree of consolidation of soil below the embankment centre and shoulder is different due to three-dimensional loading conditions. Since the increase of excess pore pressure is equal to the increase in total mean stress based on an elastic assumption, the consolidation problem along a failure surface can be considered as if the total mean stress, $\Delta\sigma_m = \gamma_{fill} H I_q$, is applied over the construction period. The different approaches given to one- and three-dimensional loading conditions are applying the total embankment load, $\gamma_{fill} H$, to the soil below the embankment centre versus applying the partial embankment load, $\gamma_{fill} H I_q$, in terms of mean stress to the soil along the potential slip surface. Therefore, the average degree of consolidation, $\overline{U}_f$, can be calculated using eqs. [8]–[10] and the consequent strength gain, Δs_{uf}, can be calculated by

Fig. 15. Vertical embankment loading on a semi-infinite mass (modified from Poulos and Davis 1974).

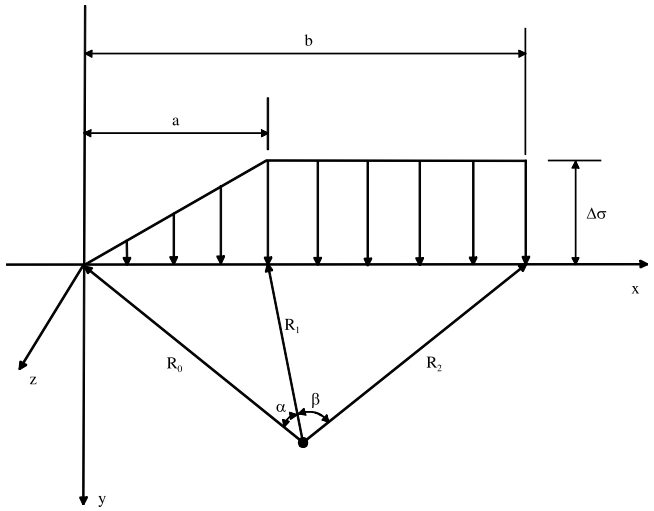

$$[13] \quad \Delta s_{uf} = [\beta(\sigma'_{mi} + \gamma_{fill} H I_q \bar{U}_f)] - s_{uo}$$

where σ'_{mi} is the initial effective mean stress.

It is worth noting that $\bar{U}_{O/C}$ in eq. [8] is the average degree of consolidation at time $t_{O/C}$ when effective mean stress σ'_m is equal to $\sigma'_{mp} = (1 + 2K'_0)\sigma'_p/3$ (e.g., the mean of preconsolidation stresses). The above approximation has proved to be reasonably accurate and conservative, as shown in following sections.

6. Proposed method

6.1. Procedure for combining consideration of embankment reinforcement and vertical drains

The method of analysis is based on an undrained strength analysis (USA) method suggested by Ladd (1991) and a limit state design philosophy. The steps in the procedure are outlined as follows and an example is given in the Appendix.

(1) Select the design criteria, including height (H), width (B), and slope (n) of the embankment; average degree of consolidation ($\bar{U}$) required; available time (t) to achieve $\bar{U}$; and construction rate (CR).

(2) Select soil parameters for the embankment fill and foundation, including undrained shear strength (s_u) profile; preconsolidation pressure (σ'_p) and current vertical effective stress (σ'_v) with depth; coefficient of lateral earth pressure at rest (K'_0) profile; normalized shear strength for soil in its normally consolidated state (s_u/σ'_m, where σ'_m is the effective mean stress for soil in its normally consolidated state); coefficient of consolidation of soil in overconsolidated ($C_{O/C}$) and normally consolidated ($C_{N/C}$) states; ratio of hydraulic conductivity in the horizontal direction (k_h) to that in the vertical direction (k_v) for undisturbed soil; ratio of hydraulic conductivity of undisturbed soil (k_h) to that of disturbed soil (k_s); length (H_d) of the longest drainage path in the vertical direction; and friction angle (ϕ) and unit weight (γ_{fill}) of the embankment fill.

(3) Select a prefabricated vertical drain system whose configuration is described by the drain spacing (S); the effective diameter (D_e) of the drain influence zone ($D_e = 1.05S$ for a triangular pattern and $1.13S$ for a square pattern); the length (L) of a single drain (equal to the thickness of clayey deposits in most cases); the diameter of the smear zone (d_s) caused by drain installation; and the equivalent diameter (d_w) and discharge capacity (q_w) of a single drain.

(4) Calculate the average degree of consolidation at the available time t using eqs. [8]–[10]. If the calculated average degree of consolidation is less than the required $\bar{U}$, repeat step 3 to select a new PVD configuration (e.g., spacing S and length L) until $\bar{U}$ is met.

(5) Estimate the average influence factor I_q ($\Delta\sigma_m = \gamma_{fill} H I_q$) for the increase in total mean stress of the foundation soil along the potential slip surface using the following elastic solutions (e.g., Poulos and Davis 1974) and Fig. 15:

$$[14a] \quad \Delta\sigma_x = \frac{\Delta\sigma}{\pi}\left[\beta + \frac{x\alpha}{a} + \frac{y}{R_2^2}(x-b) + \frac{2y}{a}\ln\frac{R_1}{R_0}\right]$$

$$[14b] \quad \Delta\sigma_y = \frac{\Delta\sigma}{\pi}\left[\beta + \frac{x\alpha}{a} - \frac{y}{R_2^2}(x-b)\right]$$

where x is the distance from the embankment toe and y is the depth; and for an elastic material under plane strain conditions, R_0, R_1, and R_2 are distances as shown in Fig. 15.

$$[14c] \quad \Delta\sigma_z = \upsilon(\Delta\sigma_x + \Delta\sigma_y)$$

where υ is Poisson's ratio; therefore,

$$[14d] \quad \Delta\sigma_m = \frac{\Delta\sigma_x + \Delta\sigma_y + \Delta\sigma_z}{3}$$

$$[14e] \quad I_q = \frac{\Delta\sigma_m}{\Delta\sigma}$$

(6) Calculate the average degree of consolidation along the potential slip surface at the end of the embankment construction, $\bar{U}_f$.

(7) Estimate the average strength increase, Δs_{uf}, of soil along the potential failure surface at the end of construction using eq. [13].

(8) Factor the strength of soils using partial factor f_c for the undrained shear strength of foundation soil ($s^*_u = s_u/f_c$) and f_ϕ for fill material ($\tan\phi'^* = (\tan\phi')/f_\phi$), and f_γ for the unit weight of fill ($\gamma^*_{fill} = \gamma_{fill} f_\gamma$) as appropriate.

(9) Factor Δs_{uf} using partial factor f_c ($\Delta s^*_{uf} = \Delta s_{uf}/f_c$).

(10) Using a limit equilibrium method, calculate the equilibrium ratio (ERAT) of restoring moment to overturning moment for the embankment without reinforcement using the factored soil parameters of embankment fill and factored undrained shear strength profile, including the strength gain during construction, i.e., $s^*_u + \Delta s^*_{uf}$; reinforcement is not needed if ERAT ≥ 1.0 and is needed if ERAT < 1.0, in which case continue with steps 11 and 12.

(11) Use a limit equilibrium program designed for the analysis of reinforced embankments (e.g., REAP; Mylleville and Rowe 1988) to calculate the required reinforcement tensile force, T_{req}, using the new factored undrained shear strength profile obtained in step 10 (T_{req} is the force required

Table 2. Calculated ERAT of reinforced embankments obtained using the proposed method.

J (kN/m)	ε_{all} (%)	T (kN/m)	CR (m/month)	H (m)	$\overline{U}_f$ (%)	Δs_u (kPa)	ERAT (-)
Soil A							
One-stage construction							
1000	5	50	2	3.70	30.80	1.37	0.914
1000	7	70	2	4.18	29.10	1.70	0.893
2000	5	100	2	4.41	28.70	1.92	0.920
2000	7	140	2	5.04	27.40	2.42	0.903
1000	5	50	1	4.17	35.20	2.80	0.932
2000	5	100	1	4.96	34.80	3.94	0.955
Two-stage construction (H_1 = 3.5 m, 4 months stoppage)							
2000	5	100	2	5.63	38.20	5.82	0.960
Soil B							
One-stage construction							
1000	5	50	4	5.75	38.00	3.76	0.945
2000	5	100	4	6.48	37.10	4.62	0.955
1000	5	50	8	5.28	35.00	2.39	0.937
2000	5	100	8	5.87	33.80	2.93	0.951
Two-stage construction (H_1 = 6 m, 1 month stoppage)							
2000	5	100	4	8.58	40.30	8.92	0.904

to give an overturning moment = restoring moment based on factored soil properties, i.e., ERAT = 1).

(12) Choose an allowable strain, ε_{all}, for the reinforcement and then the required reinforcement tensile stiffness is calculated as

$$[15] \quad J_{req} = \frac{T_{req}}{\varepsilon_{all}}$$

In this procedure, the limit states examined involve failure of the embankment, foundation, and reinforcement. All calculations except the slope stability analysis can be done by hand or using a spreadsheet program. This approach can be made equally applicable to a stage construction sequence by adding the consolidation during stoppage in steps 4 and 6, keeping other steps the same. Design parameters (e.g., S, L, T_{req}, and J_{req}) can be obtained iteratively from steps 1–12. In the design iteration, the construction rate and stage sequences can be varied such that the design grade can be achieved in an optimum time schedule. To assure embankment stability during construction, it is essential to monitor the development of reinforcement strains, excess pore pressures, settlement, and horizontal deformations and to confirm that measured values are consistent with the design values.

6.2. Comparison of the results using finite element analyses and the proposed method

Using the proposed method, the equilibrium ratio (ERAT) of restoring moment to overturning moment at the end of construction for the embankments analyzed in the previous section can be calculated. A number of cases with different reinforcement construction rates and construction stages are reanalyzed using the proposed method and are given in Table 2, where T is the tensile force developed in the reinforcement at an allowable strain ε_{all}. The embankment should have an ERAT of 1 at height H, which was calculated from finite element analyses in previous sections. ERAT in Table 2 is in the range of 0.89–0.96. It is shown that the proposed method is conservative for both one-stage construction and two-stage construction and compares well with finite element analysis results for the cases examined. Compared with that predicted by the finite element analyses, the shear strength gain along the failure surface predicted using eq. [13] is conservative. For example, the average shear strength gains predicted using eq. [13] for the embankments H = 4.41 m over soil A and H = 6.48 m over soil B are 1.92 and 4.62 kPa, respectively (see Table 2). These values are less than those calculated using finite element analyses (see Fig. 12).

7. Recommendations and conclusions

The performance of embankments constructed using prefabricated vertical drains (PVDs) and geosynthetic reinforcement has been theoretically examined. A tentative design procedure has been developed to consider the benefits arising from the use of both PVDs and reinforcement. The following conclusions are based on the analyses reported herein.

Partial consolidation of the foundation soil during embankment construction is significant because of the drainage improvement provided by prefabricated vertical drains and foundation soils usually become normally consolidated at the end of embankment construction. Consequently, the shear strength gain of soft foundation soil due to partial consolidation can substantially improve the stability of embankments such as those examined. The rate of increase in shear strength of foundation soil is a function of construction rate for a particular reinforced embankment and PVD system. Where PVDs are installed, the strength gain is relatively uniform throughout the thickness of the deposit and can be reasonably predicted using the proposed method. For a foundation installed with PVDs, the embankment design based on assuming undrained conditions and neglecting the shear strength increase in the foundation soil during construction is too conservative.

The construction rate significantly affects embankment stability and deformation. For each case, there is a unique

threshold construction rate below which reinforcement is not needed and the foundation will not experience bearing capacity failure, even for a relatively high embankment. The spacing of PVDs significantly influences the degree of consolidation at the end of embankment construction, but the effect of well resistance of typical vertical drains is insignificant. The proposed eq. [8] reasonably well predicts the average degree of consolidation when the soil moves from its overconsolidated state to a normally consolidated state under an embankment loading.

Reinforcement can substantially increase the stability of embankments under partially drained conditions when the construction rate is greater than the threshold rate. The benefit of the increase in shear strength due to partial consolidation is enhanced by the use of reinforcement. For a foundation under partially drained conditions, very high reinforcement strains may be developed due to plastic deformations of foundation soils under relatively high embankments that can be constructed because of the beneficial effects of both reinforcement and partial consolidation during construction. It was found that the embankment failure height (based on limit state design considerations) is generally governed by the allowable strain of reinforcement when the bearing capacity of foundation soil ceases to be a problem due to shear strength gain during construction.

With two-stage construction, construction of the embankment as high as possible by the use of reinforcement in the first stage results in the best performance due to the higher effective stress increase in foundation soil that is achieved during consolidation. Therefore, the use of reinforcement has the potential to allow embankment construction in a shorter period of time than that what might be required for a case without reinforcement. Since stability and consolidation are interrelated, reinforcement and PVDs should be treated together in design.

The proposed method for estimating the consolidation and consequent strength gain of foundation soil during and after construction under embankment loading proved to be conservative and reasonably accurate for the relatively uniform foundation deposits examined. The proposed method can consider both prefabricated vertical drains and reinforcement and appears to warrant further investigation as a means of preliminary design of embankments involving the use of reinforcement and PVDs. It is recommended that any such design be combined with monitoring to confirm that the performance (e.g., excess pore pressures) is consistent with that deduced in the design. A parametric study can be carried out using the proposed method to optimize the configuration of reinforcement and vertical drains.

Acknowledgement

The research reported in this paper was funded by the Natural Sciences and Engineering Research Council of Canada.

References

Barron, R.A. 1948. Consolidation of fine-grained soils by drain wells. Transactions of the American Society of Civil Engineers, **113**: 718–743.

Bassett, R.H., and Yeo, K.C. 1988. The behaviour of a reinforced trial embankment on soft shallow foundations. *In* Proceedings of the International Geotechnical Symposium on Theory and Practice of Earth Reinforcement, Fukuoka, Kyushu, Japan. A.A. Balkema, Rotterdam, pp. 371–376.

Biot, M.A. 1941. General theory of three-dimensional consolidation. Journal of Apply Physics, **12**: 155–164.

Bolton, M.D. 1986. The strength and dilatancy of sands. Géotechnique, **36**(1): 65–78.

Bonaparte, R., and Christopher, B.R. 1987. Design and construction of reinforced embankments over weak foundations. Transportation Research Record 1153, pp. 26–39.

Carrillo, N. 1942. Simple two- and three-dimensional cases in the theory of consolidation of soils. Journal of Mathematics and Physics, **21**: 1–5.

Carter, J.P., and Balaam, N.P. 1990. AFENA — a general finite element algorithm: users manual. School of Civil and Mining Engineering, University of Sydney, Sydney, NSW, Australia.

Chai, J., and Bergado, D.T. 1993. Performance of reinforced embankment on Muar clay deposit. Soils and Foundations, **33**(4): 1–17.

Chai, J.C., Miura, N., Sakajo, S., and Bergado, D.T. 1995. Behavior of vertical drain improved subsoil under embankment loading. Soils and Foundations, **35**(4): 49–61.

Chen, W.F., and Mizuno, E. 1990. Nonlinear analysis in soil mechanics — theory and implementation. Elsevier, New York.

Cheung, Y.K., Lee, P.K.K., and Xie, K.H. 1991. Some remarks on two and three dimensional consolidation analysis of sand-drained ground. Computers and Geotechnics, **12**(1): 73–87.

Fowler, J., and Edris, E.V., Jr. 1987. Fabric reinforced embankment test section, Plaquemine Parish, Louisiana, USA. Geotextiles and Geomembranes, **6**(1): 1–31.

Fowler, J., and Koerner, R.M. 1987. Stabilization of very soft soils using geosynthetics. *In* Proceedings of the Geosynthetic '87 Conference, New Orleans, Vol. 1, pp. 289–299.

Hansbo, S. 1981. Consolidation of fine-grained soils by prefabricated drains. *In* Proceedings of the 10th International Conference on Soil Mechanics and Foundation Engineering, Stockholm, Vol. 3, pp. 677–682.

Hird, C.C., and Kwok, C.M. 1990. Parametric studies of the behaviour of a reinforced embankment. *In* Proceedings of 4th International Conference on Geotextiles, Geomembranes and Related Products, The Hague, Vol. 1, pp. 137–142.

Hird, C.C., Pyrah, I.C., and Russell, D. 1992. Finite element modelling of vertical drains beneath embankments on soft ground. Géotechnique, **42**(3): 499–511.

Hird, C.C., Pyrah, I.C., Russell, D., and Cinicioglu, F. 1995. Modelling the effect of vertical drains in two-dimensional finite element analyses of embankments on soft ground. Canadian Geotechnical Journal, **32**: 795–807

Holtz, R.D. 1987. Preloading with prefabricated vertical strip drains. Geotextiles and Geomembranes, **6**(1–3): 109–131.

Holtz, R.D., Jamiolkowski, M.B., Lancellotta, R., and Pedroni, R. 1991. Prefabricated vertical drains: design and performance. CIRIA Ground Engineering Report: Ground Improvement. Butterworth-Heinemann Ltd., Oxford, U.K.

Humphrey, D.N., and Holtz, R.D. 1987. Reinforced embankments — a review of case histories. Geotextiles and Geomembranes, **6**(4): 129–144.

Industrial Fabrics Association International. 1999. 2000 Specifier's Guide. Geotechnical Fabrics Report, **17**(9).

Ingold, T.S. 1982. An analytical study of geotextiles reinforced embankments. *In* Proceedings of the 2nd International Conference on Geotextiles, Las Vegas, Vol. 3, pp. 683–688.

Jamiolkowski, M., Lancellotta, R., and Wolski, W. 1983. Precompression and speeding up consolidation: general report. *In* Proceedings of the 8th European Conference of Soil Mechanics, Helsinki, Vol. 3, pp. 1201–1226.

Janbu, N. 1963. Soil compressibility as determined by oedometer and triaxial tests. *In* Proceedings of the European Conference on Soil Mechanics and Foundation Engineering, Wiesbaden, Vol. 1, pp. 19–25.

Jewell, R.A. 1982. A limit equilibrium design method for reinforced embankments on soft foundations. *In* Proceedings of the 2nd International Conference on Geotextiles, Las Vegas, Vol. 4, pp. 671–676.

Kjellman, W. 1948. Accelerating consolidation of fine-grained soils by means of cardboard wicks. *In* Proceedings of the 2nd International Conference on Soil Mechanics and Foundation Engineering, Rotterdam, pp. 302–305.

Koerner, R.M. 1994. Designing with geosynthetics. 3rd ed. Prentice-Hall, Inc., Englewood Cliffs, N.J.

Ladd, C.C. 1991. Stability evaluation during staged construction. Journal of Geotechnical Engineering, **117**(4): 540–615.

Ladd, C.C., and Foott, R. 1974. New design procedure for stability of soft clays. Journal of the Geotechnical Engineering Division, ASCE, **100**(GT7): 763–786.

Leroueil, S., and Rowe, R.K. 2001. Embankments over soft soil and peat. *In* Geotechnical and geoenvironmental engineering handbook. *Edited by* R.K. Rowe. Kluwer Academic Publishers, Norwell, Mass., pp. 463–499.

Leroueil, S., Tavenas, F., Mieussens, C., and Peignaud, M. 1978. Construction pore pressures in clay foundations under embankments. Part II: generalized behaviour. Canadian Geotechnical Journal, **15**: 65–82.

Leshchinsky, D. 1987. Short-term stability of reinforced embankment over clayey foundation. Soils and Foundations, **27**(3): 43–57.

Li, A.L. 2000. Time dependent behaviour of reinforced embankments on soft foundations. Ph.D. thesis, The University of Western Ontario, London, Ont.

Li, A.L., and Rowe, R.K. 1999*a*. Reinforced embankments and the effect of consolidation on soft cohesive soil deposits. *In* Proceedings of the Geosynthetics '99 Conference, Boston, Vol. 1, pp. 477–490

Li, A.L., and Rowe, R.K. 1999*b*. Reinforced embankments constructed on foundations with prefabricated vertical drains. *In* Proceedings of the 52nd Canadian Geotechnical Conference, Regina, Sask., pp. 411–418.

Li, A.L., and Rowe, R.K. 2000. Reinforced embankments constructed with prefabricated vertical drains: analysis and implications for design. Research Report GEOT-12-00, Faculty of Engineering Science, The University of Western Ontario, London, Ont.

Lockett, L., and Mattox, R.M. 1987. Difficult soil problems on Cochrane Bridge finessed with geosynthetics. *In* Proceedings of the Geosynthetic '87 Conference, New Orleans, Vol. 1, pp. 309–319.

McGown, A., Andrawes, K.Z., Mashhour, M.M., and Myels, B. 1981. Strain behaviour of soil–fabric model embankments. *In* Proceedings of the 10th International Conference on Soil Mechanics and Foundation Engineering, Stockholm, Vol. 3, pp. 739–744.

Mesri, G., and Rokhsar, A. 1974. Theory of consolidation for clays. Journal of the Geotechnical Engineering Division, ASCE, **100**(GT8): 889–904.

Mylleville, B.L.J., and Rowe, R.K. 1988. Simplified undrained stability analysis for use in the design of steel reinforced embankments on soft foundations. Research report GEOT-3-88, Faculty of Engineering Science, The University of Western Ontario, London, Ont.

Olson, R.E. 1977. Consolidation under time dependent loading. Journal of the Geotechnical Engineering Division, ASCE, **103**(GT1): 55–60.

Olson, R.E., and Ladd, C.C. 1979. One-dimensional consolidation problems. Journal of the Geotechnical Engineering Division, ASCE, **103**(GT1): 55–60.

Poulos, H.G., and Davis, E.H. 1974. Elastic solutions for soil and rock mechanics. Wiley, New York.

Rixner, J.J., Kraemer, S.R., and Smith, A.D. 1986. Prefabricated vertical drains. Vol. 1: engineering guidelines. U.S. Federal Highway Administration, Report FHWA-RD-86/168.

Rowe, R.K. 1984. Reinforced embankments: analysis and design. Journal of Geotechnical Engineering, ASCE, **110**(GT2): 231–246.

Rowe, R.K. 1997. Reinforced embankment behaviour: lessons from a number of case histories. *In* Proceedings of the Symposium on Recent Developments in Soil and Pavement Mechanics, Rio de Janeiro. *Edited by* M. Almeida. A.A. Balkema, Rotterdam, pp. 147–160

Rowe, R.K., and Li, A.L. 1999. Reinforced embankments over soft foundations under undrained and partially drained conditions. Geotextiles and Geomembranes, **17**(3): 129–146.

Rowe, R.K., and Soderman, K.L. 1987*a*. Stabilization of very soft soils using high strength geosynthetics: the role of finite element analyses. Geotextiles and Geomembranes, **6**(1–3): 53–80.

Rowe, R.K., and Soderman, K.L. 1987*b*. Reinforcement of embankments on soils whose strength increases with depth. *In* Proceedings of the Geosynthetics '87 Conference, New Orleans, pp. 266–277.

Rowe, R.K., MacLean, M.D., and Barsvary, A.K. 1984. The observed behaviour of a geotextile-reinforced embankment constructed on peat. Canadian Geotechnical Journal, **21**: 289–304.

Rowe, R.K., Gnanendran, C.T., Landva, A.O., and Valsangkar, A.J. 1995. Construction and performance of a full-scale geotextile reinforced test embankment, Sackville, New Brunswick. Canadian Geotechnical Journal, **32**: 512–534.

Russell, D. 1990. An element to model thin, highly permeable materials in two dimensional finite element consolidation analyses. *In* Proceedings of the 2nd European Specialty Conference on Numerical Methods in Geotechnical Engineering, Santander, Spain, pp. 303–310.

Schiffman, R.L. 1958. Consolidation of soil under time-dependent loading and varying permeability. Highway Research Board, Proceedings of the Annual Meeting, **37**: 584–617.

Schimelfenyg, P., Fowler, J., and Leshchinsky, D. 1990. Fabric reinforced containment dike, New Bedford superfund site. *In* Proceedings of the 4th International Conference on Geotextiles, Geomembranes and Related Products, The Hague, Vol. 1, pp. 149–154.

Sharma, J.S., and Bolton, M. 1996. Centrifuge modelling of an embankment on soft clay reinforced with a geogrid. Geotextiles and Geomembranes, **14**(1): 1–17.

Taylor, D.W. 1948. Fundamentals of soil mechanics. Wiley, New York.

Yoshikuni, H., and Nakanodo, H. 1974. Consolidation of soils by vertical drains with finite permeability. Soils and Foundations, **14**(2): 35–46.

Zeng, G.X., and Xie, K.H. 1989. New development of the vertical drain theories. *In* Proceedings of the 12th International Conference on Soil Mechanics and Foundation Engineering, Rio de Janeiro, Vol. 2, pp. 1435–1438.

Zhu, G.F., and Yin, J.-H. 1998. Consolidation of soil under depth-dependent ramp load. Canadian Geotechnical Journal, **35**: 344–350.

Zhu, G.F., and Yin, J.-H. 1999. Consolidation of double soil layers under depth-dependent ramp load. Géotechnique, **49**(3): 415–421.

Appendix: A worked example

(1) Select design criteria — A 4.5 m high four-lane highway embankment with a 28 m wide crest and side slope of 2:1 (h:v) is constructed over a soft foundation deposit. The average degree of consolidation $\bar{U}$ of the foundation soil must reach 90% within a 9 month period of time by the use of prefabricated vertical drains. The construction conditions allow a construction rate of 4 m/month.

(2) Soil parameters — Foundation soil B and the embankment fill described in Sect. 3.1. are used for this example. The undrained shear strength, vertical effective stress, and preconsolidation pressure profiles are shown in Fig. 2*b*. The average foundation soil parameters are σ'_{vo} = 50.8 kPa, σ'_m = 37.3 kPa, σ'_p = 73.6 kPa, σ'_{mp} = 54 kPa, s_{uo} = 20.9 kPa, $C_{O/C} = 2.32 \times 10^{-3}$ m^2/h, and $C_{N/C} = 3.86 \times 10^{-4}$ m^2/h. The other required soil parameters are $K'_0 = 0.6$, $\alpha = s_u/\sigma'_p = 0.31$, $\beta = s_u/\sigma'_{mp} = 0.423$, $k_h/k_v = 3$, $k_h/k_s = 3$, and H_d = 7.5 m. The embankment fill material has $\phi = 37°$ and γ_{fill} = 20 kN/m^3.

(3) Select prefabricated vertical drain system — The configuration of the PVD system is given as S = 2 m (a square pattern), D_e = 2.26 ($D_e = 1.13S$ for square pattern), L = 15 m, d_w = 0.066 m, q_w > 100 m^3 /a, and d_s = 0.264 m (the diameter of the smear zone caused by drain installation is four times the equivalent diameter of the vertical drain).

(4) Calculate the average degree of consolidation in the available time, t = 9 months, using eqs. [8]–[10] — The time at the end of construction for the 4.5 m high embankment at a rate of 4 m/month is 810 h (~34 days). Assuming an embankment load of $\Delta\sigma = 4.5 \times 20 = 90$ kPa, the average degree of consolidation required to bring the vertical stress to the preconsolidation pressure (from 50.8 to 73.6 kPa) is $\bar{U}_{O/C}$ = (73.6 – 50.8)/90 = 0.253. Using eqs. [9] and [10] and $C_{O/C}$, the back-calculated $t_{O/C}$ is 472 h for soil to reach $\bar{U}_{O/C}$ = 25.3%. Then t'_C = 810 – 472 = 338 h; using eqs. [9] and [10] and $C_{N/C}$, the calculated $\bar{U}_{N/C}$ is 88.7% at t = 9 months. Using eq. [8], the total average degree of consolidation is $\bar{U}$ = 0.253 + (1.0 – 0.253) × 0.887 = 0.916 = 91.6%, which is greater than that required. Therefore, the configuration of PVDs is satisfactory. Continue to the next step.

(5) Estimate the average influence factor I_q — The influence factor I_q for total mean stress at a number of locations along the potential slip surface in the foundation soil is calculated using eq. [14]. The average I_q is 0.48.

(6) Calculate the average degree of consolidation along the potential slip surface ($\bar{U}_f$) at the end of construction using eqs. [8]–[10] — This step is similar to step 4. The total mean stress load, $\Delta\sigma_m = \gamma_{fill} H I_q$ = 20 × 4.5 × 0.48 = 43.2 kPa, is applied in a time of 810 h. The required average degree of consolidation $\bar{U}_{O/C}$ is 39% to bring the initial mean stress σ'_m = 37 kPa to the mean preconsolidation pressure σ'_{mp} = 54 kPa. Using eqs. [9] and [10] and $C_{O/C}$, the back-calculated $t_{O/C}$ is 186 h. Using eqs. [9] and [10] and $C_{N/C}$, the calculated $\bar{U}_{N/C}$ is 5.8% at t = 9 months. Using eq. [8], the calculated $\bar{U}_f$ is 42.5%.

(7) Calculate the average strength increase of soil along the potential failure surface at the end of construction using eq. [13] — The average strength increase $\Delta s_{uf} = [\beta(\sigma'_m + \gamma_{fill} H I_q \bar{U}_f)] - s_{uo} = 0.423 \times (37.3 + 20 \times 4.5 \times 0.48 \times 0.425) - 20.9 = 2.65$ kPa.

(8) Factor strength of soils using partial factor f_c = 1.3 for undrained shear strength profile (s^*_u) and f_ϕ = 1.2 for fill material (ϕ^* = 32°) and f_γ = 1.0 for unit weight of fill (γ^*_{fill} = 20 kN/m^3).

(9) Factor Δs_{uf} using partial factor f_c = 1.3, giving Δs^*_{uf} = 2.04 kPa.

(10) Using the limit equilibrium program REAP (Mylleville and Rowe 1988) and the new factored undrained shear strength profile ($s^*_u + \Delta s^*_{uf}$), the calculated minimum ERAT is 0.74 for the embankment without reinforcement. Since ERAT < 1.0, reinforcement is needed and therefore continue to steps 11 and 12.

(11) Using REAP, the calculated required reinforcement tensile force, T_{req}, is 160 kN/m to maintain a minimum ERAT of 1.0.

(12) Choose an allowable strain of ε_{all} = 5% for the reinforcement. The required reinforcement tensile stiffness is calculated using eq. [15] to be J_{reg} = 3200 kN/m (or two layers of reinforcement that will develop 160 kN/m at 5% strain).